# A benchmark analysis of subcooled heat transfer in a novel half-unit-cylinder-head for verifying in-vehicle engine evaporative cooling under dynamic conditions

**M. Langari, J. F. Dunne, S. Jafari, J-P Pirault, Z. Yang*, C. A. Long, and J. Thalackottore Jose**
Department of Engineering and Design, University of Sussex, UK.
*Department of Engineering, College of Engineering and Technology, University of Derby, UK



**Abstract**

Evaporative cooling (EC) is a potentially attractive method of thermal management in highly downsized engines. As a benchmark for robust EC system development, a novel half-unit-cylinder-head has been designed to study the heat transfer achievable with evaporative cooling strategies under realistic hot metal conditions with an appropriate coolant flow field. Multi-phase computational fluid dynamics (CFD) and conjugate heat transfer (CHT) analysis are performed under subcooled flow boiling conditions to achieve both the design requirements for the hot-side surfaces and the specification of heating arrangements. Analysis is undertaken to ensure that thermal diffusion and flow conditions are representative of coolant flow in highly-boosted IC engines. The CFD model predictions show good correlation with available experimental data for both heat flux and metal temperatures in a typical downsized pressure-charged spark-ignition engine cylinder head.

## 1 INTRODUCTION

Progressive trends in downsizing and pressure-charging spark ignition engines have resulted in increasingly high thermal loads. Consequently, high heat rejection rates are needed to avoid operation at dangerously elevated engine metal temperatures. This trend has pushed conventional (single phase) cooling systems to their absolute limit of being able to achieve efficient engine thermal management and temperature control. Reaching this limit has justified further fundamental research on alternative cooling strategies. Evaporative cooling (EC) is a potentially attractive strategy owing to: 1) the high rates of heat transfer available from the coolant phase change during boiling, and 2) from the significant functional advantages that a robustly-controlled EC system can potentially provide. However, despite extensive research to date, no closed-loop evaporation-based IC engine cooling system has been successfully implemented on a production vehicle owing presumably to unsolved technical challenges and insufficient evidence of successful operation at representative engine test conditions.

Predictions of both heat transfer and the associated flow field in the presence of coolant phase-change is of significant importance in the development of downsized

internal combustion engines. In a typical downsized internal combustion engine, heat rejection to the cooling system must take place at rates of order 1.2 MW/m$^2$. With such high heat transfer rates, boiling may be unavoidable in some regions under certain coolant flow conditions. Subcooled boiling has been attractive in engine cooling system applications [1]–[4] where the high heat transfer rates of nucleate boiling may be utilised without use of extra components (e.g. a vapour separator and condenser). For safe operation, and to achieve optimised design of the engine and cooling system, it is crucial to accurately predict the heat transfer rates and vapour fractions within the coolant passages.

Despite extensive research on the phenomenon, nucleate boiling heat transfer mechanism is still not fully understood, and thus a fundamental model without empirical correlations is yet to be developed. Computational Fluid Dynamics, together with mechanistic or empirical boiling models, is a viable tool to provide thermal predictions of nucleate boiling flows. Several experimental and numerical studies have examined the heat transfer regimes leading to the nucleate boiling. Boiling flow however involves various events e.g. bubble nucleation, growth, detachment, coalescence, collapse, and condensation that occur on different space and time scales, making boiling a complex phenomenon. Owing to unknown characteristics of nucleation sites, mechanistic models based on bubble formation and departure phenomena, are not yet able to predict the nucleate boiling heat transfer. Empirical correlations are therefore more often used in practical situations. The boiling correlation of Kandlikar [5] describes subcooled boiling flow of ethylene-glycol-water mixtures in engine-like geometries. It is however mainly developed for heat transfer estimation in fully-developed boiling regime and is known to perform poorly in the nucleate boiling transition region [6]. The correlations of Rohsenow [7] and Chen [8] describe the total heat flux as a combination of a convective component and a nucleate boiling component providing predictions in both fully convective and boiling region. These models have been widely used in automotive applications [6], [9]–[11]. Robinson *et al.* [9] emphasized the significance of accurate prediction of the (single phase) convective component for reliable overall heat transfer estimations in both convective and boiling regimes. Appropriate thermal boundary layer and vapour formation modelling is also known to play a significant role in accurate predictions of heat transfer in the boiling regime [12]–[15].

As part of an extensive research study to address underlying EC system challenges a novel experimental rig has been designed. At the heart of this rig is a representative half-unit-cylinder-head which is being used to study the heat transfer achievable with evaporative cooling strategies under realistic conditions. In particular, the half-unit-cylinder-head can be excited dynamically (with a shaker) to provide measurements of evaporative-cooling system thermal performance in the presence of vibration levels and frequencies typical of a boosted IC engine in a vehicle on the road. Extensive computational fluid dynamics (CFD) simulation is being undertaken to assist the rig design and to understand the performance of both evaporative-cooling strategies, and the conventional cooling systems that they could replace. In this paper, multi-phase CFD and conjugate heat transfer (CHT) analysis of this half-unit-cylinder-head model is examined under subcooled flow boiling conditions. This is to serve as a benchmark for robust EC system development under realistic engine conditions. The study focuses on the thermal conditions for both the coolant and hot-gas sides which is needed for hot-side surface design and for gas heating specification. Simulations are performed by means of the finite-volume CFD solver STAR-CCM+ (version 10) where the VOF (Volume-of-Fluid) algorithm [16] is adopted to capture the liquid-vapour interface. The paper is structured as follows. First, the modelling approach is presented. Then the CFD simulations are described and a comparison made against experimental data.

## 2 GEOMETRY AND BOUNDARY CONDITIONS

An exhaust-side "half-unit-cylinder-head" model has been designed based on consideration of: i) very high steady-state heat-flux capability, ii) the flow-path representation of the cylinder head, iii) curved and arcuate internal coolant jacket surfaces, iv) the feasibility of optical access, and v) matching the temperature gradients of downsized engines. The current design is intended to represent a highly-boosted downsized engine (with 71.4 mm bore and 82 mm stroke). The use of a half cylinder is intended to focus on the highest heat flux zones of a cylinder head and to reduce the mass of the shaken parts of the test rig to enable higher amplitudes and frequencies to be excited as part of assessing the impact of the vibration and agitation on evaporative cooling. The model comprises a central half-unit-cylinder-head piece with a conventional coolant jacket as shown in Figure 1.

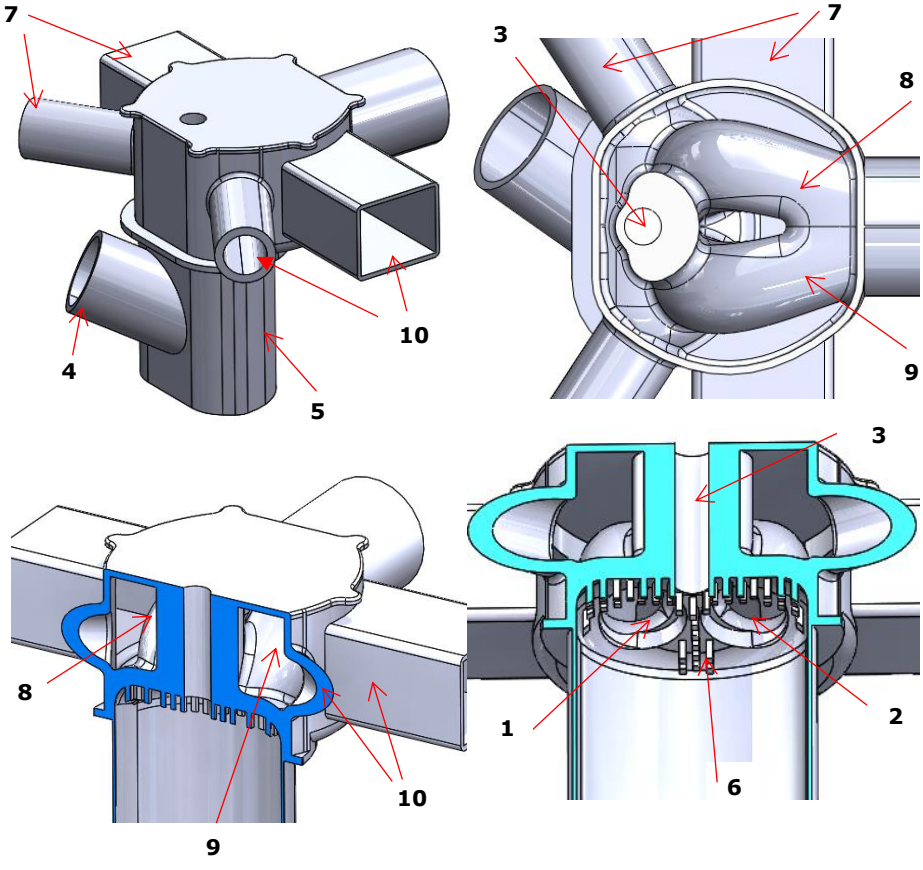


1-2: Exhaust ports openings
3: Spark plug boss
4: Gas by-pass port
5: Gas heater shroud
6: pin fins
7: Coolant inlet
8-9: Exhaust ports
10: Coolant outflow

**Figure 1. 'Half-unit-cylinder-head' model showing upper observation plate, conventional cooling jacket, and square heating fins (of dimension 2 mm × 2 mm × 6 mm) on the flame face**

There is an uppermost access plate to allow observation and instrumentation, and for eventual use of targeted coolant sprays. The half-unit-cylinder head has three gas-flow paths, i.e. one through the exhaust ports (1 and 2, Figure 1), one through the spark plug boss (3, Figure 1), and a by-pass (4, Figure 1) - all three with throttle controls. Heating on the rig will be achieved using a propane gas burner. The appropriate heat flux levels and three dimensional gradients on the gas face are achieved with 68 distributed pin fins (i.e. No. 6 on Figure 1). Coolant flow arrives via conduit (7, Figure 1) to the exhaust ports (8 and 9, Figure 1) zones. Figure 2 shows the flow-ports and corresponding flow-paths.

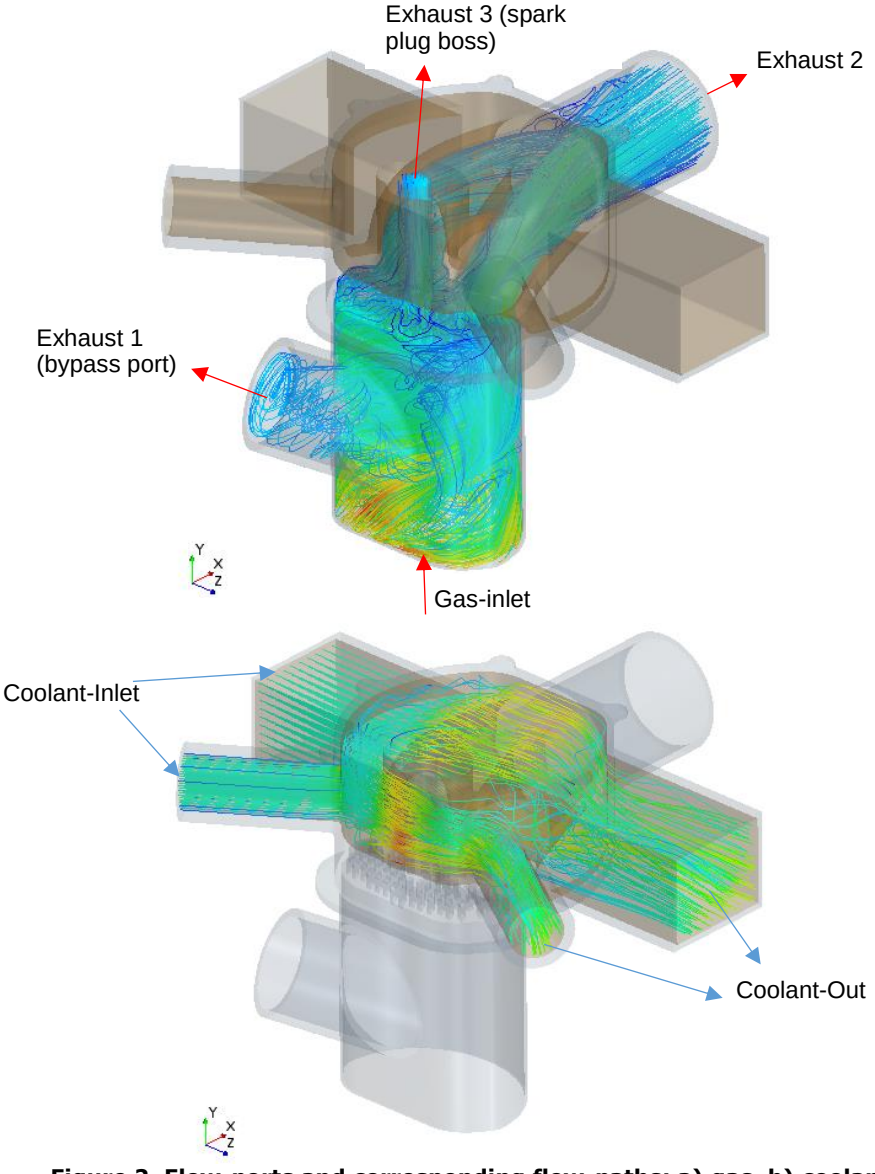


**Figure 2. Flow-ports and corresponding flow-paths; a) gas, b) coolant streamlines**

The boundary conditions adopted are based on available data relevant to highly-boosted downsized engine operating conditions. The metal properties are set for Aluminium alloy with specific heat 900.0 J/kg-K, and thermal conductivity of 150.0 W/m-K. The fluid domain is a mixture of water and ethylene glycol with 50% volumetric ratios. The coolant inlet is assumed to be 1.225 kg/s at 90°C, based on an assumed value of 1.35 l/s total pump flowrate for a typical 3-cylinder engine. Coolant outlet takes place through outflow boundaries as shown in Figure 2 (Part 10 in Figure 1). These flow outlets will be used selectively to reproduce the flow patterns in the engine cylinder head. Using empirical estimates, 2.4 kW heat transfer through the flame face of one whole unit of a cylinder head at rated power, is envisaged at the rated power of 33.3 kW per cylinder for a fuel energy rate of 103.4 kW. The hot side fin design and hot gas flow conditions were optimised for local heat-flux, representative metal temperature gradients, and integrated heat energy rates. The hot gas inlet flow into the canister (Part 5 in Figure 1) of 0.00214 kg/s at 1970°C is prescribed which corresponds to gas heating with a 6 kW propane heater (given propane enthalpy of combustion 46.1 MJ/kg and stoichiometric air/fuel ratio of 15.5). A swirling effect, to increase heat transfer to the pin fins, is added to the gas inlet boundary by defining the flow direction vector as (*r, theta, z*), for example = (0.1, 0.8, 0.1) in Figure 3. Zero outlet flow to the bypass port, Exhaust 1, is prescribed at the targeted load condition. Atmospheric pressure outlet is imposed on exhaust ports 2-3.

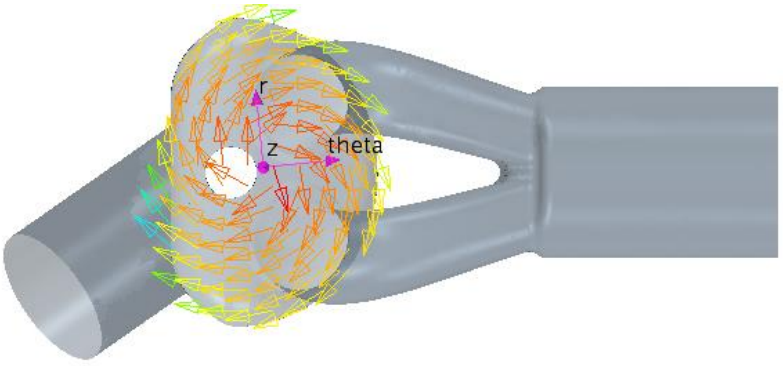


**Figure 3. Swirling flow on the gas inlet; flow direction vector (*r, theta, z*): (0.1, 0.8, 0.1)**

## 3 NUMERICAL FRAMEWORK

A steady-state three-dimensional CFD/CHT case with separate fluid, gas and solid regions (interfacing) is used in the analysis presented here. Liquid and vapour flow are simulated using the VOF Multiphase modelling approach within the Eulerian framework [16]. A homogeneous flow model is employed where liquid and vapour bulk properties are defined separately. The governing equations are solved for the mixture flow with shared velocity, pressure, and temperature field assumed to be the same for the two phases. An additional transport equation for the phase volume fraction is solved to obtain the spatial phase concentrations within the domain. Changes in density due to the phase change are therefore taken into account without solving two sets of governing equations for the liquid and vapour phases. The convective part of heat flux is given by:

$$q_c = h_c(T_w - T_c) \tag{1}$$

and

$$h_c = \frac{\rho C_p u_\tau}{T^+|_{y^+(y_c)}} \tag{2}$$

where $h_c$ is the convective heat transfer coefficient, $T_w$ is the wall temperature, $T_c$ is the local near wall cell temperature, $\rho$ and $C_p$ are density and specific heat of the mixture respectively, $u_\tau$ is the friction velocity, $T^+$ is the dimensionless temperature, $y_c$ is the normal distance of the near wall cell, and $y^+$ is the dimensionless wall distance $u_\tau y_c / v_f$.

The implemented phase change model accounts for the onset of boiling through the use of sub-models. The heat transfer at the wall-fluid boundary is used to calculate the phase change mass transfer rate (evaporation or condensation). The vapour phase temperature is assumed constant at the saturation temperature $T_{sat}$ and the liquid temperature is approximated to the mixture temperature T. The total heat interchange between the liquid and vapour phases is then used to work out the mass transfer between phases:

$$\dot{m}_{ec} = \frac{C_{HTC\times Area}(T - T_{sat})}{h_{fg}} \tag{3}$$

where $C_{HTC\times Area}$ is the heat transfer coefficient between the vapour bubbles and adjacent liquid multiplied by the contact area between the two phases, and $h_{fg}$ is the phase change enthalpy. Boiling occurs at the liquid-solid interface where $T_w > T_{sat}$ and the surface heat flux due to boiling is calculated by the empirical correlation of Rohsenow [7]:

$$q_{bw} = \mu_f h_{fg} \sqrt{\frac{g(\rho_f - \rho_g)}{\sigma}} \left( \frac{c_{p,f}(T_w - T_{sat}}{C_{qw} h_{fg} Pr_f^{1.7}} \right)^{3.03} \tag{4}$$

where $\mu_f$, $c_{p,f}$, $Pr_f$ are the dynamic viscosity, the specific heat, and the Prandtl number of the liquid phase respectively, g is gravitational acceleration, $\rho_f$ is the density of the vapor phase, $\sigma$ is the surface tension at the liquid-vapour interface, $T_w$ is the wall temperature and $C_{qw}$ is an empirical coefficient, the value of which depends on the liquid-surface (and surface finish) combination. A value of 0.0028 was used in the current study as being representative of engine coolant and aluminium alloy. The vapour mass flow rate per unit area, through boiling on the wall, then follows from:

$$\dot{m}_{ew} = \frac{C_{ew} q_{bw}}{h_{fg}} \tag{5}$$

where $C_{ew}$ is the model constant indicating how much of the boiling heat flux is used for vapour generation.

Liquid and vapour phases are treated as a mixture where one set of turbulent equations are solved for the mixture phase. Steady-state RANS computations were undertaken using the *k-ε* turbulence model with "All $y^+$" wall treatment approach of STAR-CCM+ for near-wall turbulence quantities - a hybrid wall treatment combining high $y^+$ wall treatment for coarse meshes, and the low $y^+$ wall treatment for fine meshes, specially formulated for meshes of intermediate resolution where the near-wall cell lies within $1 < y^+ < 30$. For $y^+ <= 1$ no wall function is used and the model assumes that the viscous sublayer is fully-resolved by the mesh. For $y^+ > 30$, the classic wall-function approach is adopted where wall shear stress, turbulent

production and dissipation are governed by the equilibrium turbulent boundary layer theory. The "All y+" method blends any turbulence quantity such as dissipation, production, stress tensor, etc. calculated by the "high-y+" approach or by the low-y+ approach using an exponential weighing function where the value for the turbulence quantity $\Phi$ is calculated as:

$$\emptyset = w\emptyset_{low} + (1 - w)\emptyset_{high} \tag{6}$$

where $w$ is given by:

$$w = exp\,(-\frac{Re_y}{11}) \tag{7}$$

and where

$$Re_y = \frac{\sqrt{k}y}{v}) \tag{8}$$

is a wall-distance-based Reynolds number, y is the normal distance from the wall to the wall-cell centroid, $v$ is the kinematic viscosity, and $k$ is the turbulent kinetic energy. Boundary layers have been resolved with appropriate near-wall prism layers according to the adopted near-wall treatment model. The near wall resolution in the current study ranges between $12 < y^+ < 25$ (i.e. a near wall cell distance between 0.1 - 0.4 mm). The computational domain is divided into three blocks and polyhedral conformal grids have been generated for the three blocks: hot gas region, aluminium half-unit-cylinder-head region, and coolant flow field region. Figure 4 shows grid cells on the hot gas and coolant blocks. A grid sensitivity study was performed using three different grid resolutions with 600000, 800000, and 910000 cells to ensure the grid resolution does not influence the solution.

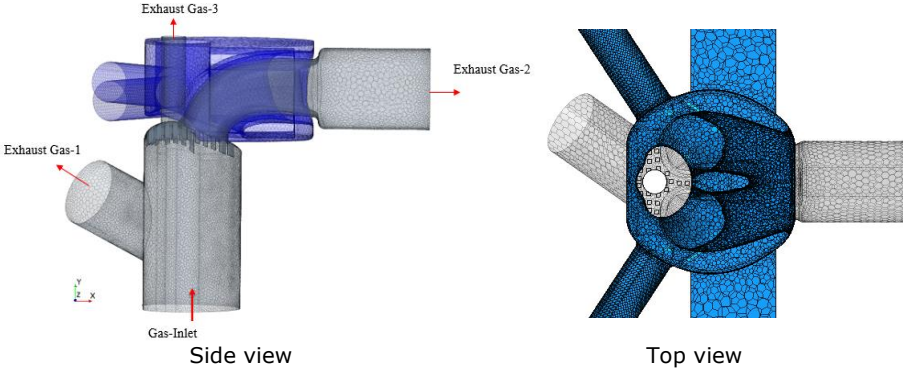


**Figure 4. Computational grids on hot gas (grey) and coolant (blue) domains**

## 4 RESULTS AND DISCUSSION

Figure 5 shows the predicted values of surface temperature on both the gas side and the coolant sides of the half-unit-cylinder-head. In these (and all subsequent results

in this section) the computations were carried out using a grid with 793,615 cells.

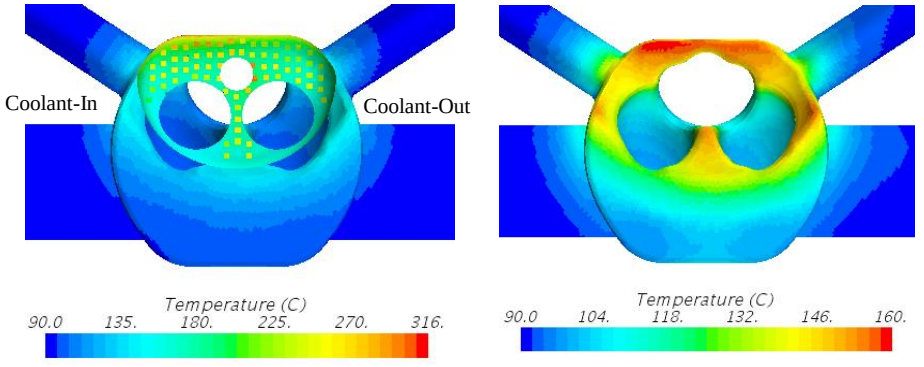


**a) Metal temperatures on gas side face** **b) Metal temperatures on coolant side face**

**Figure 5. Predicted surface temperatures on: a) the gas side, and b) the coolant side.**

In the interests of clarity, it is considered worthwhile to explain some of the geometric features in figures 5a and 5b as they will also be shown elsewhere in the paper. In Figure 5a, where the view shown looks onto the hot gas surface, the two large circular holes near the centre are the exhaust gas outlets (labelled as Exhaust Gas 2, in Figure 2). The smaller single hole above these is also an exhaust gas outlet (labelled as 3, in Figure 1). Towards the left of the figure are the coolant inlet pipes, and towards the right, the two coolant outlet pipes. Of interest in Figure 5a is the gas side face itself, which comprises the central part of the figure (mostly coloured in green). The 2mm x 2mm heating fins with a typical height of 6 mm can be seen as an array of squares on this hot gas side surface. The maximum temperature of the fins is around 300°C - but most are around 250°C. However, the temperature of the majority of the substrate at the base of the fins is in the region of 180°C to 200°C. This is consistent with the limited (measured and predicted) data available (but not shown) for a similar downsized engine. In Figure 5b, the white blanked-out section (that is also shown in Figure 1) is the spark plug boss with a conduit through it for gas heating. The two exhaust ports are indicated by the voids immediately below, and to the left, and right of this section. Although there is no measured data for comparison, the temperature distributions shown on the coolant-side do follow qualitative expectations. The maximum coolant-side surface temperatures occur in the region above the hot gas side. And within this region the highest surface temperatures occur in the vicinity of the exhaust ports (around 160°C for a bulk coolant temperature of 96°C). It is also worthy of note that there is asymmetry in the temperature field: the temperatures near Coolant-In are higher than those near Coolant-Out.

The predicted flow field, corresponding to Figure 5b, is shown in Figure 6. Coolant enters from the inlet pipe to the cylinder head via two ducts next to the exhaust ports, and then flows to the right and around the exhaust port towards the spark plug boss. The coolant flow is mainly longitudinal, from the inlet pipes on the left, to the exit pipes on the right. The maximum velocities are around 2.0 m/s but over most of the cylinder head they are typically in the region of 0.8-1.4 m/s. The reason for the asymmetry in the temperature field (noted earlier) can now be understood. This is because coolant velocities are lower towards the upper coolant inlet pipe than outflow pipe. The flow pattern and velocities depicted here are qualitatively in broad agreement with the flow pattern in a highly-boosted downsized engine where there is a longitudinal flow in the cylinder head from one cylinder to another.

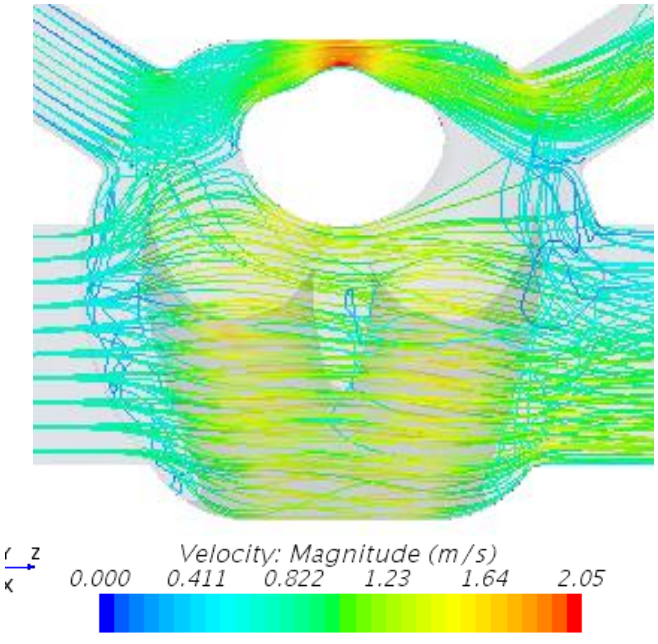


**Figure 6. Predicted flow streamlines on the coolant side**

Figure 7 shows a contour map of the predicted values of heat flux distribution on the coolant side of the half-unit-cylinder-head. In the coolant inlet and exit pipes the heat fluxes are less than $10^4$ W/m$^2$, which is lower than associated with nucleate boiling. This is to be expected since the surface temperatures here are generally below the saturation temperature and consequently the heat transfer is mostly due to single phase convection.

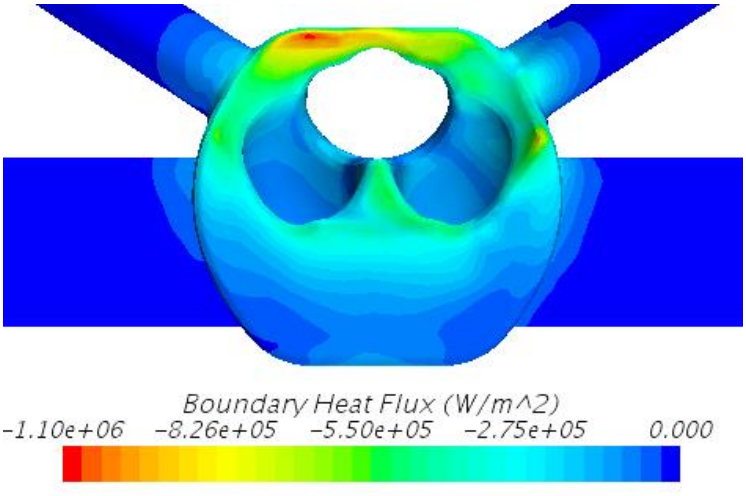


**Figure 7. Predicted values of coolant-side heat flux**

Elsewhere the heat flux is seen to vary across the cylinder head by several orders of magnitude from $10^4$ W/m$^2$ to $10^6$ W/m$^2$. These values are entirely consistent with

those occurring during nucleate boiling. It is also encouraging to note that the predicted maximum heat flux of around 1.1 x $10^6$ W/$m^2$ which occurs towards the top of the diagram of the half-unit-cylinder-head, is consistent with empirical estimates (of 1.23 x $10^6$ W/$m^2$) at this location. For the main part of the surface, the heat flux is in the region of 0.5 x $10^6$ W/$m^2$, which is also consistent with empirical estimates for downsized engines.

Figure 8 shows the predicted values of vapour quality (i.e. fraction of vapour by mass). There are localised pockets of 0.14% vapour fraction which correspond to regions with high heat flux and low coolant velocity. There are also regions of 0.05% vapour fraction in the valve bridge area.

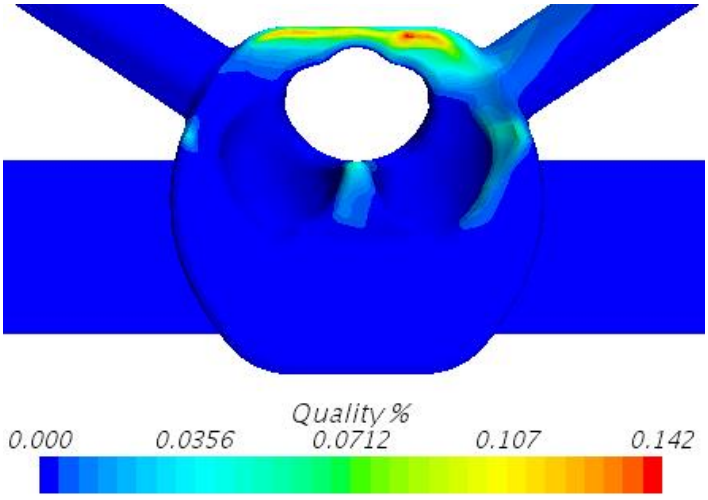


**Figure 8 Predicted values of vapour quality**

## 5 CONCLUSIONS

A simulation capability has been developed to obtain coolant flow and associated heat transfer to assist in the design of an experimental half-unit-cylinder-head test piece. This capability is to target conditions that an evaporatively-cooled version of the half-unit-cylinder-head must endure in terms of external heating and cooling, so that peak metal temperature conditions and heat flux levels emulate those found at full-load on a highly-boosted downsized engine cylinder head. Two-phase CFD/CHT simulations, allowing predictions of the temperature field for subcooled boiling conditions on the coolant side, have been used to determine the required gas heating power, and pin-type cooling fin design on the flame-face. Predicted wall temperatures, heat flux, and vapour volume fraction have been presented to confirm that the targeted heat flux on the half-unit-cylinder-head test piece can be achieved. The predicted temperatures and heat flux levels compare well with measured engine data (not shown) at a small number of available discrete points.

## ACKNOWLEDGMENTS

The authors wish to acknowledge funding support for this project from the EPSRC under Contract Number: EP/M005755/1. The technical support is also acknowledged of colleagues at Ford Dunton UK and Dearborn USA, Denso Italy, and the Ricardo Technical Centre Shoreham, UK.

**REFRENCES**


[1] A. J. Torregrosa, A. Broatch, P. Olmeda, and O. Cornejo, "Experiments on subcooled flow boiling in I.C. engine-like conditions at low flow velocities," *Exp. Therm. Fluid Sci.*, vol. 52, pp. 347–354, Jan. 2014.

[2] K. Robinson, N. a F. Campbell, J. G. Hawley, and D. G. Tilley, "A Review of Precision Engine Cooling," *SAE Tech. Pap.*, no. 1999-01–0578, 1999.

[3] N. Ap and M. Tarquis, "Innovative Engine Cooling Systems Comparison," *SAE Tech. Pap.*, no. 2005-01–1378, 2005.

[4] N. A. . Campbell, D. G. Tilley, S. A. MacGregor, and L. Wong, "Incorporating Nucleate Boiling in a Precision Cooling Strategy for Combustion Engines," *SAE Tech. Pap.*, no. 971791, May 1997.

[5] S. G. Kandlikar and M. Bulut, "An Experimental Investigation on Flow Boiling of Ethylene-Glycol/Water Mixtures," *J. Heat Transfer*, vol. 125, no. 2, p. 317, 2003.

[6] H. Steiner, G. Brenn, F. Ramstorfer, and B. Breitschadel, "Increased Cooling Power with Nucleate Boiling Flow in Automotive Engine Applications," in *New Trends and Developments in Automotive System Engineering*, InTech, 2011.

[7] W. M. Rohsenow, "A Method of Correlating Heat Transfer Data for Surface Boiling of Liquids," *Trans. ASME,* vol. 74, no. 1952, pp. 969–976, 1952.

[8] J. C. Chen, "Correlation for boiling heat transfer to saturated fluids in convective flow," *Ind. Eng. Chem. Process Des. Dev.*, vol. 5, no. 3, pp. 322–329, 1966.

[9] K. Robinson, J. G. Hawley, and N. A. F. Campbell, "Experimental and modelling aspects of flow boiling heat transfer for application to internal combustion engines," *Proc. Inst. Mech. Eng. Part D J. Automob. Eng.*, vol. 217, no. 10, pp. 877–889, Jan. 2003.

[10] M. Cardone, A. Senatore, D. Buono, M. Polcino, G. De Angelis, and P. Gaudino, "A Model for Application of Chen's Boiling Correlation to a Standard Engine Cooling System," *SAE Tech. Pap.*, no. 2008-01–1817, Jun. 2008.

[11] S. Fontanesi and M. Giacopini, "Multiphase CFD-CHT optimization of the cooling jacket and FEM analysis of the engine head of a V6 diesel engine," *Appl. Therm. Eng.*, vol. 52, no. 2, pp. 293–303, 2013.

[12] D. Carpentiero, S. Fontanesi, V. Gagliardi, S. Malaguti, S. Margini, M. Giacopini, A. Strozzi, L. Arnone, M. Bonanni, and D. Franceschini, "Thermo-mechanical analysis of an engine head by means of integrated CFD and FEM," *SAE Tech. Pap.*, no. 2007-24–0067, Sep. 2007.

[13] S. Fontanesi, D. Carpentiero, S. Malaguti, M. Giacopini, S. Margini, and L. Arnone, "A New Decoupled CFD and FEM Methodology for the Fatigue Strength Assessment of an Engine Head," *SAE Tech. Pap.*, no. 2008-01–0972, Apr. 2008.

[14] M. Shala, "Simulation of nucleate boiling flow using a multiphase mixture modelling approach," *IMA J. Appl. Math.*, vol. 77, no. 1, pp. 47–58, Feb. 2012.

[15] J. G. Hawley, M. Wilson, N. A. F. Campbell, G. P. Hammond, and M. J. Leathard, "Predicting boiling heat transfer using computational ftuid dynamics," *Proc. Inst. Mech. Eng. Part D J. Automob. Eng.*, vol. 218, no. 5, pp. 509–520, Jan. 2004.

[16] C. W. Hirt and B. D. Nichols, "Volume of fluid (VOF) method for the dynamics of free boundaries," *J. Comput. Phys.*, vol. 39, no. 1, pp. 201–225, 1981.